INHOMOGENEOUS HHYDROGEN DEFLAGRATIONS IN THE PRESENCE OF OBSTACLES IN 25 m^3 ENCLOSURE. EXPERIMENTAL RESULTS

Schiavetti, M., Carcassi, M.N.
[1] Department of Civil and Industrial Engineer, University of Pisa, Largo Lucio Lazzarino 2, PISA, 56124, ITALY, martinoschiavetti@gmail.com

ABSTRACT

Explosion venting is a frequently used measure to mitigate the consequence of gas deflagrations in closed environments. Despite the effort to predict the vent area needed to achieved the protection through engineering formulas and CFD tools, work has still to be done to reliably predict the outcome of a vented gas explosion. Blind-prediction exercises recently published show a large spread in the prediction of both engineering formula than CFD tools. University of Pisa performed experimental tests in a 25 m^3 facility in inhomogeneous conditions and with the presence of simple obstacles constituted by plates bolted to HEB beams. The present paper is aimed to share the results of hydrogen dispersion and deflagration tests and discuss the comparison of maximum peak overpressure generated with different blockage ratio and repeated obstacles sets. Description of the experimental set-up includes all the details deemed necessary to reproduce the phenomenon with a CFD tool.

1.0 INTRODUCTION

Explosion venting is a frequently used measure for mitigating the consequences of hydrogen deflagrations in confined enclosure.

Due to the high buoyancy of hydrogen, most of the real accidents that follow an unintended release in closed environments foresee an accumulation of the released gas under the canopy of the enclosure and a stratification in layers at different concentrations, instead of homogeneous mixtures.

Nevertheless, most of the experimental tests performed in the past were conducted in highly idealized conditions, namely homogeneous conditions and empty enclosures. Apart from a few experimental campaigns[1, 2], most tests were performed in homogeneous mixture. Furthermore few experimental campaigns were performed accounting for the presence of obstacles [3, 4, 5]. Recently, in the HySEA project, experimental campaigns were conducted in 12 foot ISO-containers by GexCon [6, 7] and in a small scale enclosure by University of Pisa, investigating both homogeneous than stratified mixtures in real volume applications with and without the presence of obstacles [8]. In those experimental campaigns most of the tests were performed venting through the roof.

Inside HySEA project blind predictions exercises were also performed [10, 11] to evaluate the capabilities of Engineering formulas and CFD tools to predict the outcome of hydrogen vented deflagrations in containers filled with various sets of obstacles. Results from the blind prediction study of inhomogeneous tests showed that, although several modellers predicted the stratification of hydrogen inside the container with reasonable accuracy, a large spread in results for the maximum reduced explosion pressure were predicted. Results suggests that such scenarios represented a significant challenge for modellers.

In order to provide more data to the scientific community and to the developers of CFD tools the present paper describes a series of experimental tests of hydrogen releases and deflagrations in a 25 m^3 enclosure vented through one side of the enclosure. Tests have been performed with simple shape obstacles easy to reproduce in a CFD tool. Both different blockage ratio and repeated sets of obstacles scenario have been studied.

2.0 EXPERIMENTAL SET UP

The CVE (Chamber View Explosion), see figure 1, is a nearly cubic structure characterized by an internal volume of about 25 m^3; the roof and one side face are entirely covered with glass panels. All other faces are covered with steel panels having different functions. The bottom and the side opposite the glass one are entirely made of steel strengthened panels which are not removable, while the other two lateral faces, on opposite sides, are the test vent and the safety vent respectively. The design pressure of the test facility is 35 kPa, while the safety vent has been designed to open at 30 kPa, which determines the maximum allowed internal pressure's peak.

Hydrogen was released from a pipe placed in the middle of the floor, diameter of the pipe being ¾ of an inch, a metal sponge was placed on top of the pipe to help the dispersion of the gas. Since the roof of the enclosure was made of glass panels, during sunny days the heating caused by solar radiation produced an air convective movement which was affecting to some extent the stratification of hydrogen.

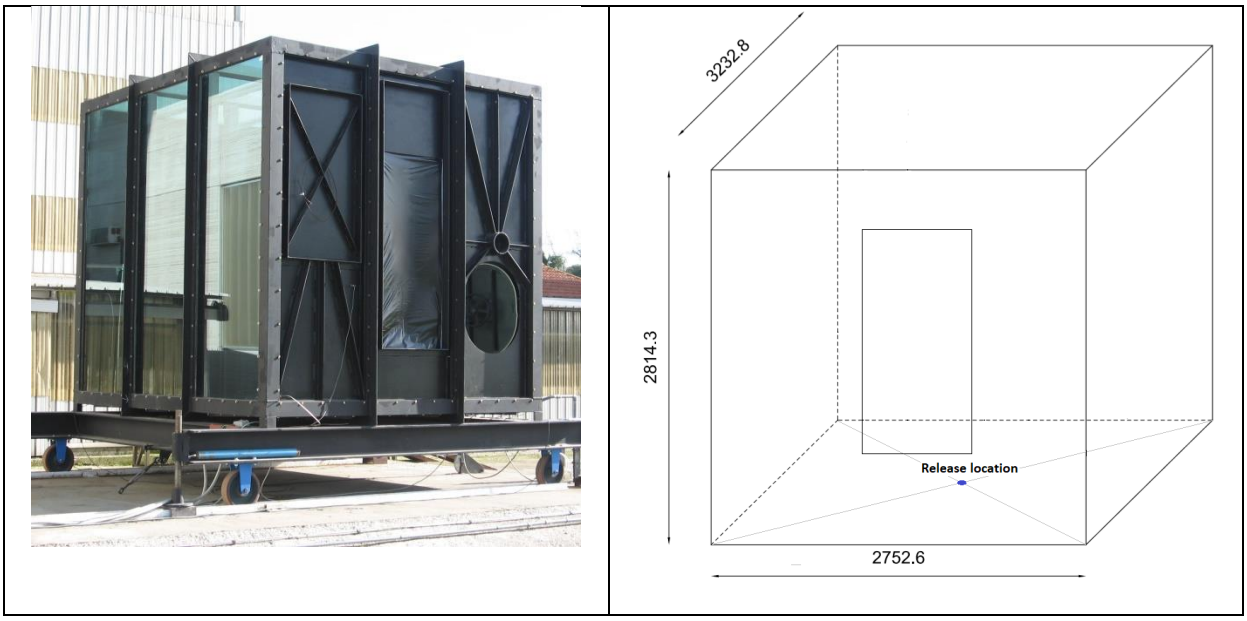

Figure 1 – Picture of the CVE test facility (left) and dimensions [mm] (right)

During the release of hydrogen the following parameters were recorded:

- Hydrogen bottles pressure and temperature,
- Hydrogen mass flow rate
- Hydrogen concentration in 5 different location inside the enclosure.

Internal atmosphere was sampled in 5 location and analysed by MSA concentration analysers having a measurement range 0-22.5% vol., data were recorded at 1Hz frequency. Three of the sampling lines were located close to the centreline of the enclosure at different heights, 2 of the sampling lines were located on the sides of the facility to check distribution of hydrogen on planes at the same height. Concentrations listed in table 1 are referred to the three sampling location on the centreline of the facility placed at 0.4m, 1.184m and 2.5m above the floor respectively. The 4^{th} and 5^{th} sampling location were changed during the experimental campaign and are different in different tests. Figure 2 shows the ignition location, the pressure transducer locations and the hydrogen concentration sampling locations close to the centreline of the enclosure.

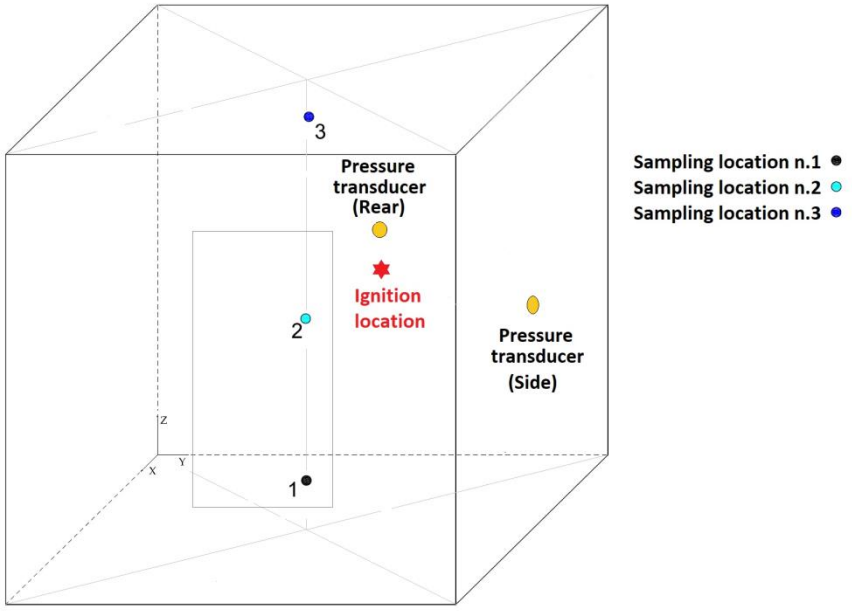

Figure 2 – Ignition, pressure transducers and internal atmosphere sampling locations

Table 1 lists the concentration sampling location coordinates, reference system being shown in figure 2.

Table 2. Concentration sampling location coordinates.

Concentration sampling point coordinates [mm]			
N.	X	Y	Z
1	1700	1440	400
2	1700	1440	1840
3	1700	1440	2500
4	Different location in every test		
5	Different location in every test		

The vent area was 1.1 m^2 in every test. Figure 3 shows the vent location and dimension.

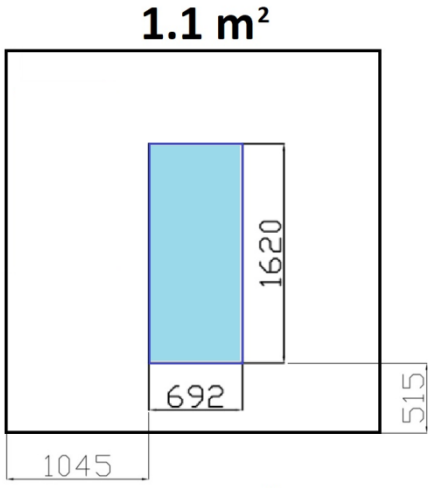

Figure 3 – Vent location and dimensions [mm]

Obstacles are constituted by flat steel plates bolted to posts. Two row of four posts were placed inside the enclosure and are always present in all the tests performed with obstacles. The posts are HEB100 steel beams welded to a basement plate bolted to the floor and anchored to the top of the enclosure. The coordinates of the HEB100 beams axis is shown in figure 4, the lateral beams are adherent to the sides of the enclosure. Steel plates can be bolted to the posts, they have dimension of 850x850 mm and thickness 5 mm. The upper edge of the top plate is distant 150 mm from the top of the enclosure. In the tests included in the present paper plates were placed between the two central beams of each row as shown on the right side of figure 4.

In the following discussion the 1st set of obstacles refers to beams and plates closer to the ignition location, while the 2nd set of obstacles refers to beams and plates closer to the vent.

Figure 4 shows the location of the posts (left side) and a 3D view of one row of obstacles with plates bolted two the central beams (right side).

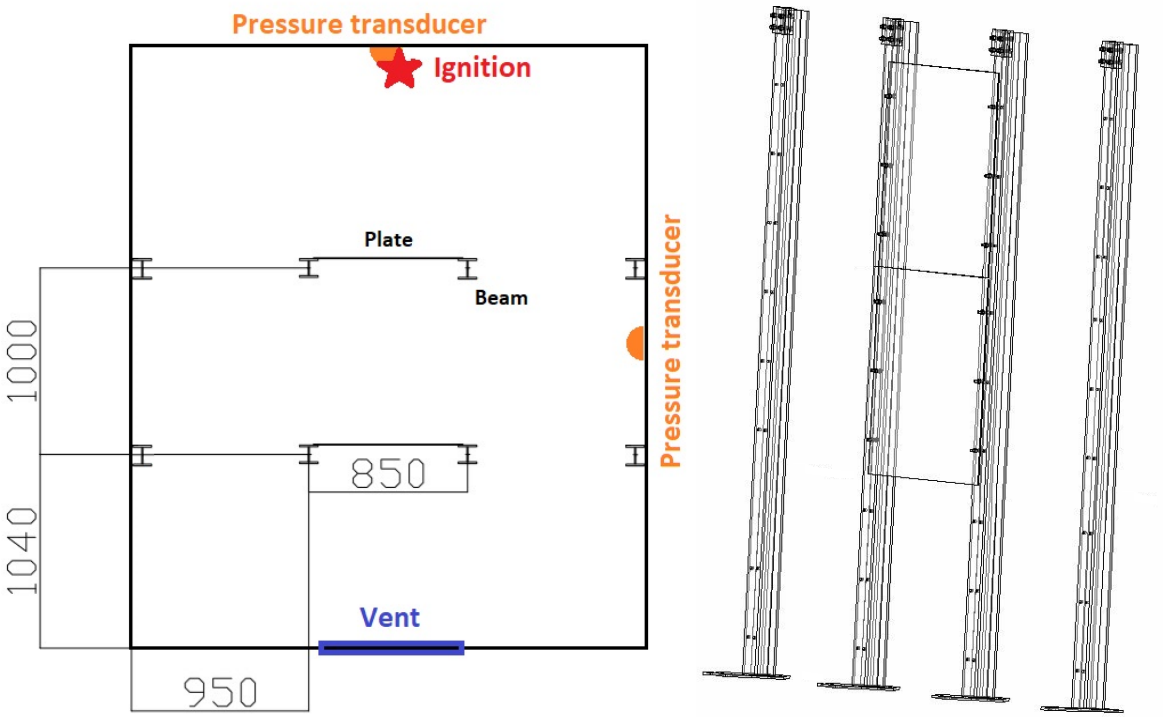

Figure 4 – Top view of the enclosure with indication of HEB axis coordinates [mm] and 3D view of one row of obstacles

Figure 5 shows the different obstacle configurations of the test included in this article.

The upright posts occupy 14.5% of the cross section of the enclosure, 1 plate and the posts occupy 23.4% of the cross section, 2 plates and the posts occupy 32.3% of the cross section.

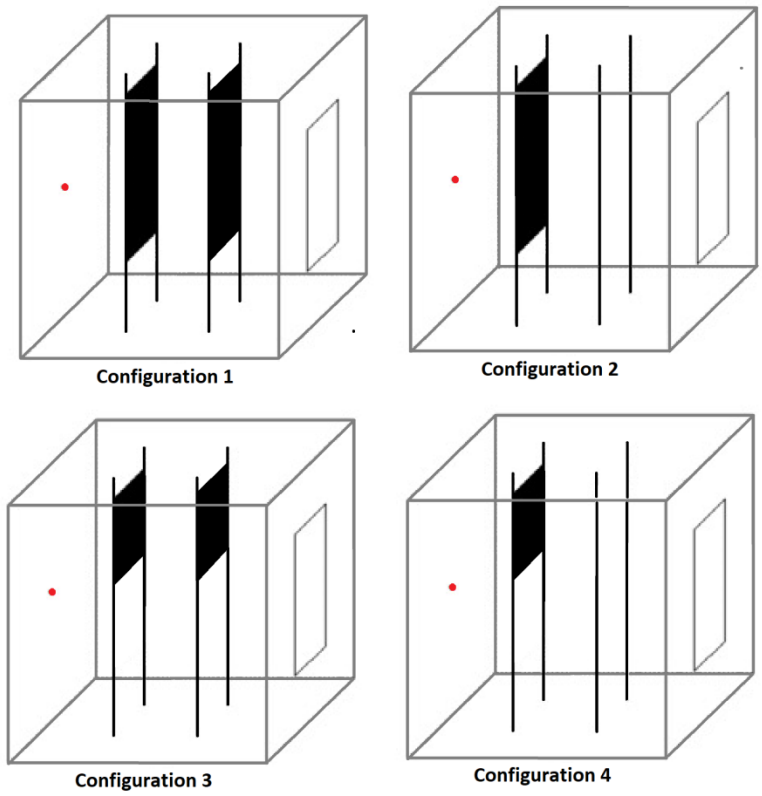

Figure 5 – Obstacle configurations

The ignition system consisted of an electrode connected to a remote driven circuit and designed to prevent accidental sparks. For all the tests included in this paper the ignition was located in the middle of the wall opposite the vent area. Table 2 lists the ignition coordinates, the reference system being shown in figure 2.

Table 2. Ignition coordinates, reference .

Ignition coordinates [mm]			
N.	X	Y	Z
1	20	1450	1060

Overpressure inside the enclosure was measured by two pressure transducer. One pressure transducer was located in the middle of the wall opposite the vent (Rear), the second was located in the middle of the lateral wall opposite the glass one (Side). During the deflagration pressure data were recorded at a frequency of 5 KHz. During the deflagration the ignition was prompted 2 seconds after starting to record the reading of the pressure transducers. Pressure time history will be presented in time range 2-4 seconds, where the origin of the graphs will represent the time at which the ignition was given.

Some of the tests were performed with injection of salty water spray performed before the hydrogen release. Salty water spray allowed to video record the flame by recording the visible field emission of salt. For the video recording were used 2 commercial PAL video cameras with 25 frame per second. The standard recording foresee the acquisition of the odd and even lines in two consecutive temporal intervals of 1/50 seconds, this allowed the video analysis at 50 frame per second with lower image quality.

Table 3 lists the tests included in this paper. Total mass of hydrogen released, mass flow rate and internal temperature of the enclosure are provided as well as the recorded hydrogen concentrations at 3 different heights on the centreline of the enclosure before the ignition.

Table 3. Lists of experimental tests and H_2 release and distribution characteristics.

Test ID	**Obst. conf.**	**T_{CVE} [°C]**	**H_2 released [g]**	**Flow rate [g/s]**	**H_2 conc. h=0.4 m**	**H_2 conc. h= 1.84 m**	**H_2 conc. h=2.5 m**
VAT40	None	24	261	0.61		12.1	
VAT41	None	25	255.6	0.63	1 (*)	14 (**)	16.7 (***)
ISP07	1	24	172	0.62	6.6 (****)	10.1	13.6
ISP08	1	26	217,5	0.675	2.8	12.8	16.2
ISP10	1	32	200	0.72	2	12	15.2
ISP11	3	34	178	0.705	1.4	11.4	14.5
ISP12	3	32	219.5	0.73	3	13.6	16
ISP13	3	27	191.5	0.74	1.8	11.6	14.8
ISP14	3	34	193	0.69	2	11.8	15.1
ISP15	3	36	218.5	0.67	3.4	13.4	16.1
ISP19	4	35	172,5	0.71	1.4	11.2	14.2
ISP20	4	36	212.5	0.715	3.6	13.2	16.3
ISP21	4	26	180	0.66	2	13.6	14.5
ISP22	4	34	217	0.7	3.4	12.2	16
ISP23	4	20	219,5	0.73	2	12.2	15.8
ISP24	2	21	219,5	0.73	2	12.2	15.8

NOTE:
(*) h=0.2 m
(**) h = 1.36 m
(***)h = 1.58 m
(****) h=0.87m

3.0 RESULTS AND DISCUSSION

In table 4 the peak overpressure recorded during the vent opening and the maximum peak pressure of the tests included in this paper are listed.

Table 4. Lists of experimental tests and measured peak overpressure.

Test ID	Vent opening pressure [kPa]	Maximum peak overpressure [kPa]
VAT40	2.0	4.9
VAT41	2.1	8.0
ISP07	2.6	6.8
ISP08	2.9	19.5
ISP10	2.6	12
ISP11	2.2	5.2
ISP12	2.3	15
ISP13	2.6	5.3
ISP14	2.2	6.6
ISP15	2.7	10.5
ISP19	2.5	2.6
ISP20	2.6	7.7
ISP21	2.7	3
ISP22	2.7	6.9
ISP23	2.6	6
ISP24	2.6	8,1

Hydrogen release and stratification were found to be repeatable, see figure 6, although the contemporary presence two sets of plaets affected the hydrogen distribution on the longitudinal planes. Particularly, being the release located in the middle of the two sets of obstacles, the contemporary presence of the plates on both the obstacles sets, produced higher concentration in the locations on the centreline of the enclosure with respect to the tests were only one set of obstacle was present.

Figure 6 shows the concentration-time history of the three locations on the centreline of the enclosure at different heights recorded during the release of hydrogen in tests ISP23 and ISP24. During the release, the concentration analyser which sampling location was 0.4m above the release hole, reached its saturation concentration, approximately 22.5%vol., represented by the flat line in figure 6.

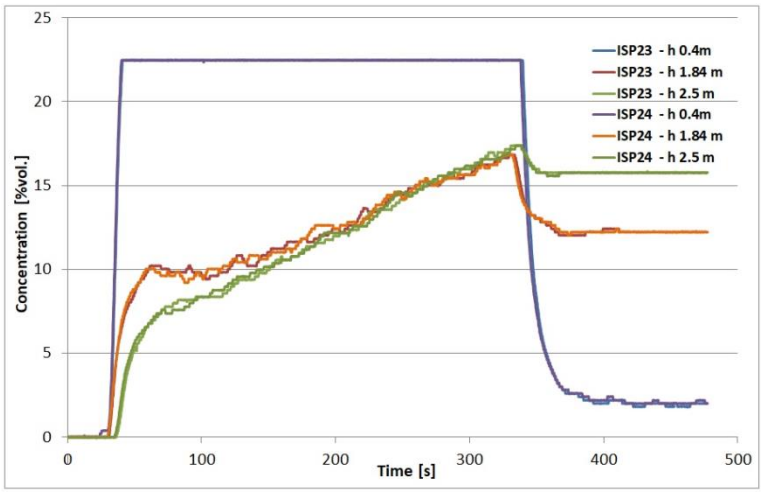

Figure 6 – Hydrogen concentration-time history for tests ISP23 and ISP24

Pressure-time history recorded during the deflagrations show a first peak generated by the vent opening, than a second peak achieved when the flame front reaches the vent area. The opening pressure of the plastic sheet ranged between 2.2 and 2.7 kPa. The average opening pressure being slightly higher in tests with obstacles with respect to tests performed with the empty enclosure. A possible explanation for this behaviour being that the presence of the obstacles between the flame front in its initial stage and the vent reduces the dynamic pressure acting on the plastic sheet.

Before the second peak two "steps" are present in the pressure-time history, the first of the two often showing a brief decrease on pressure, the second characterized by a drop in pressure increase rate or dp/dt, see left side of figure 7. These two "steps" were also present in pressure-time histories of tests performed with the empty enclosure in homogeneous conditions, see right side of figure 7, they may be associated with progressive opening of the plastic sheet which breaks when the first peak is recorded but is than completely removed only later during the progress of the deflagration.

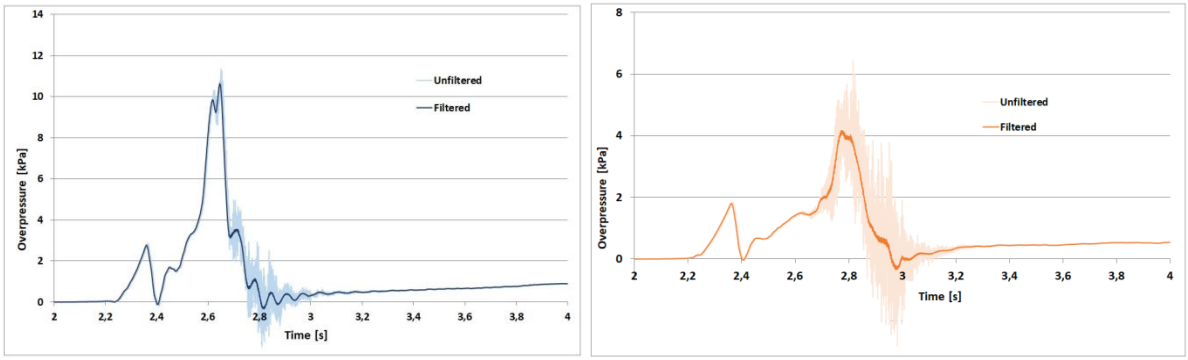

Figure 7 – P-T history for inhomogeneous deflagration with obstacles ISP15 (left) and homogeneous deflagration in the empty enclosure (right)

After the second peak, a third peak is present in some tests, associated with pressure oscillations. The flame acoustic interaction is deemed responsible of the third peak. As reported in the literature by several authors, in the presence of obstacles flame-acoustic interaction is not as strong as for the empty enclosure. The lower strength of flame acoustic interaction during vented deflagration in the presence of obstacles has been confirmed by the present experimental campaign.

Maximum achieved overpressure increased consistently with increasing mass of hydrogen released for all tested configurations. This seemed reasonable since, despite the stratification, all the tests involved lean hydrogen mixtures

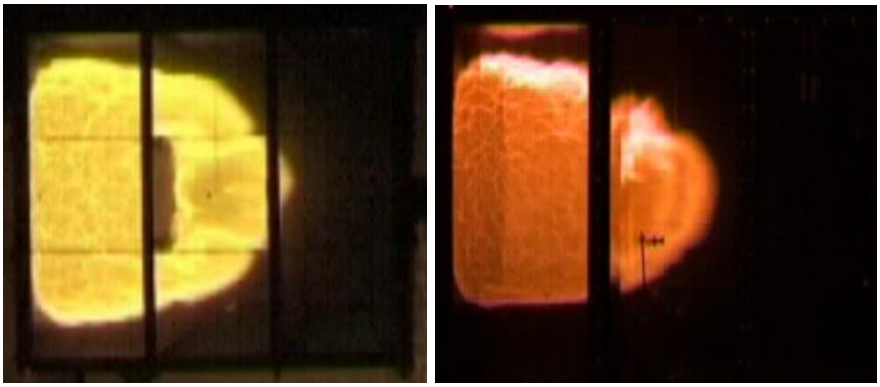

Figure 8 – Flame front passing the obstacle, top view (left) and front view (right). Test ISP23.

Figure 8 shows a frame from the video recorded during the deflagration one of the tests with obstacle configuration 4, during the moment when the flame front hits and is propagated through the first set of

obstacles. On the left side the video frame is taken from camera showing the top view of the enclosure, on the right side the video frame is taken from the camera showing the front view. The flame front is propagated following the vortex generated by flow field around the two sides and the bottom of the plate.

Figure 9 shows a frame from the video recorded during the deflagration in test ISP24, obstacle configuration 2, during the moment when the flame front hits and is propagated through the first set of obstacles. The flame front is propagated following the vortex generated by flow field around the two sides of the plates, in this case, being 2 plates present, the flame front propagate mostly from the 2 sides and only later under the plates.

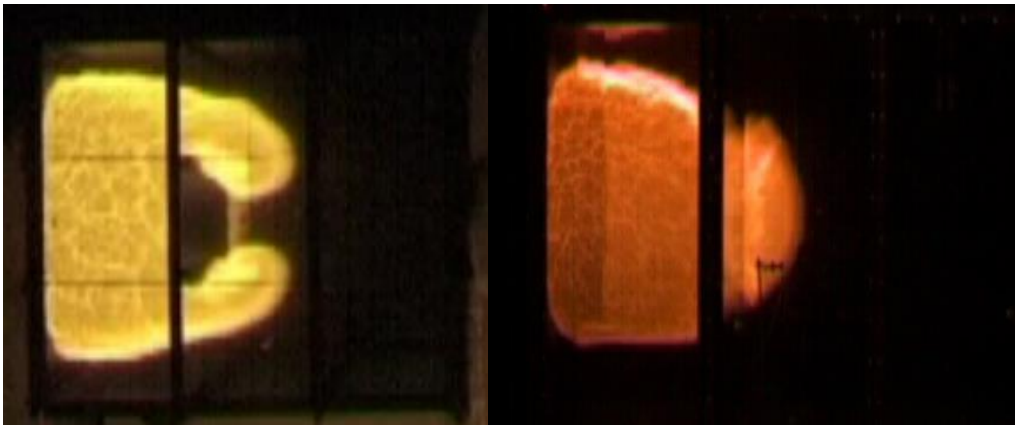

Figure 9 – Flame front passing the obstacle, top view (left) and front view (right). Test ISP24.

Maximum peak pressure achieved for the same amount of hydrogen released and similar achieved stratification increases when increasing the blockage ratio.

Figure 10 shows a comparison between the pressure time history achieved in tests ISP23, blockage ratio 23.4%, and ISP24, blockage ratio 32.3%. The two tests were performed with identical hydrogen stratification as shown in figure 6.

The comparison shows an identical history in the first stage of the deflagration, than the peak overpressure is higher for the test with higher blockage ratio.

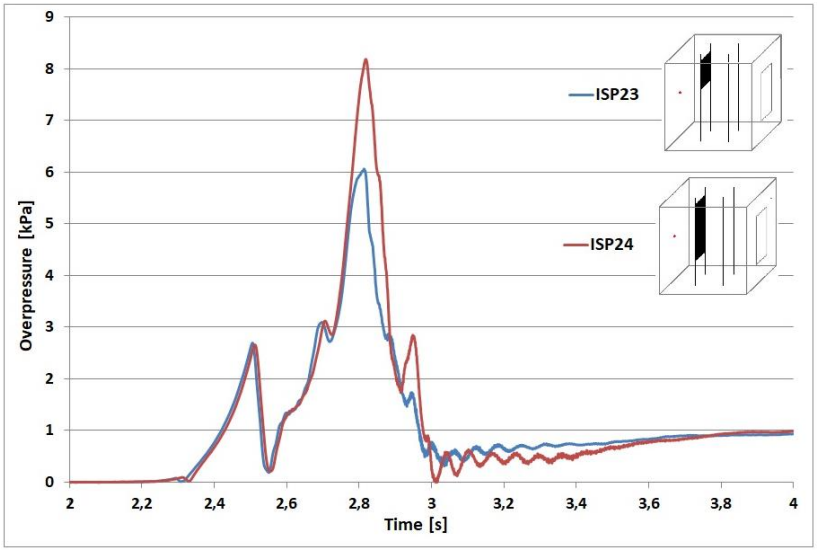

Figure 10 – Filtered pressure-time history for tests ISP23 and ISP24

The maximum peak pressure increases also doubling the obstacles. In the configurations under investigation the increase of overpressure produced by repeated obstacles is higher than the one produced by the increased blockage ration. While increasing the blockage ration from 1 plate (23.4% of the section) to 2 plates (32.3% of the section) increase the maximum achieved overpressure of around 30%, doubling the obstacles produced a more than doubled overpressure.

Figure 11 shows a comparison of the filtered pressure-time history obtained in the configuration with one set and 2 sets of obstacles. In the configuration with one plate in the top position the presence of the second set of obstacles increased the maximum peak overpressure form 6.9 to 15 kPa. In the configuration with two plates in the central and top position the presence of the second set of obstacles increased the maximum peak overpressure form 8.1 to 19.5 kPa.

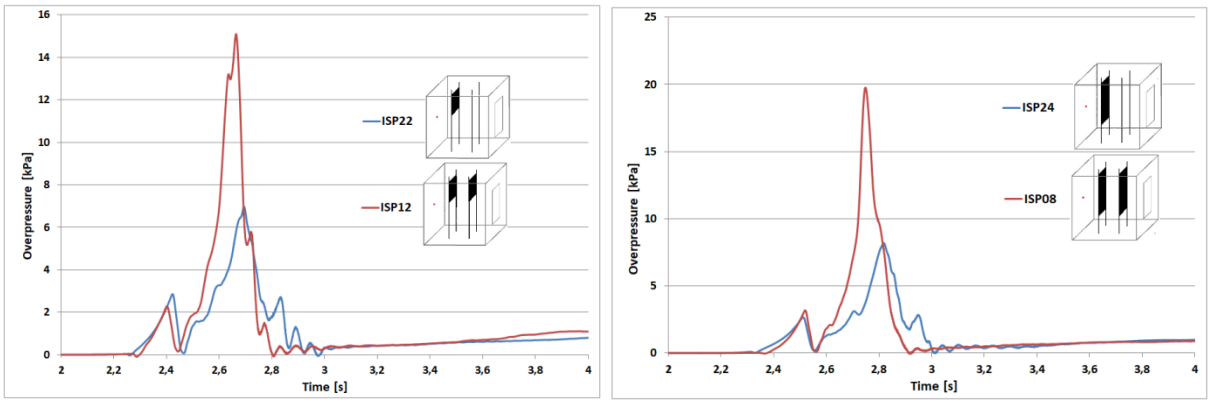

Figure 11 – Comparison of P-T history of tests with 1 and 2 sets of obstacles

Figure 12 shows the maximum peak pressure achieved with the tested obstacle configurations as a function of the mass of hydrogen released.

In homogeneous conditions the amount of hydrogen released would correspond to an average concentration between 8 and 10% vol. In the empty enclosure and for the selected vent area the maximum peak pressure achieved in homogeneous condition for hydrogen concentration between 8%vol. and 10%vol. would not exceed the vent opening pressure. Overpressure generated by a larger amount of hydrogen released, correspondent to and average concentration of around 12% vol., would generate a maximum peak pressure of 4.9 kPa in homogeneous and 8 kPa in inhomogeneous conditions respectively.

Results show that deflagration performed in idealized conditions may underestimate the maximum peak pressure achieved in real condition where hydrogen is stratified and obstacles are present.

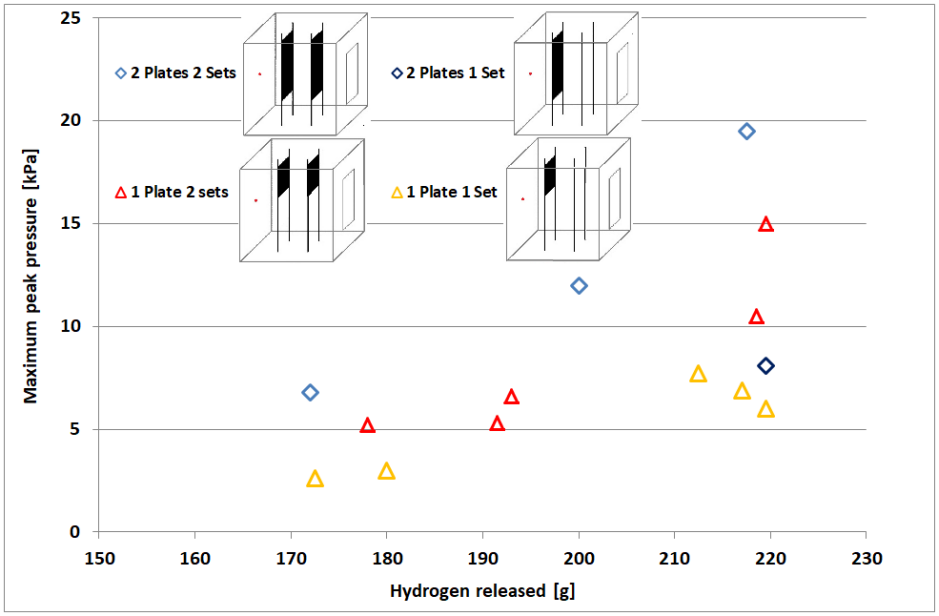

Figure 11 – Maximum peak pressure as a function of the mass of hydrogen released

4.0 CONCLUSIONS

Inhomogeneous hydrogen deflagration tests have been performed by the University of Pisa in the presence of obstacles. Different blockage ratio and repeated obstacles were investigated.

Results show that increasing the blockage ratio the maximum overpressure achieved increases. The effect of repeated obstacles on the increase of maximum peak pressure is even higher than the increase in blockage ratio. For the same amount of hydrogen released deflagration performed in idealized conditions underestimate the maximum peak pressure achieved in real condition where hydrogen is stratified and obstacles are present.

Results have been presented including all the details considered sufficient for modelers to reproduce gas dispersion and deflagration by CFD tools.

REFERENCES

1. M. Kuznetsov, A. Friedrich, G. Stern, N. Kotchourko, S. Jallais, B. L'Hostis, Medium-scale experiments on vented hydrogen deflagration, Journal of Loss Prevention in the Process Industries Volume 36, Pages 416-428 https://doi.org/10.1016/j.jlp.2015.04.013
2. D.Makarov, P.Hooker, M.Kuznetsov, V.Molkov, Deflagrations of localised homogeneous and inhomogeneous hydrogen-air mixtures in enclosures, International Journal of Hydrogen Energy, Volume 43, Issue 20, 17 May 2018, Pages 9848-9869
3. Schiavetti M., Carcassi M. "Maximum overpressure vs. H2 concentration non-monotonic behavior in vented deflagration. Experimental results" International Journal of Hydrogen Energy Volume 42, Issue 11, 16 March 2017, Pages 7494-7503, http://dx.doi.org/10.1016/j.ijhydene.2016.03.180.
4. C.R.Bauwens, J Chao, S.B. Dorofeev, Effect of hydrogen concentration on vented explosion overpressures from lean hydrogen–air deflagrations, International Journal of Hydrogen Energy, Volume 37, Issue 22, November 2012, Pages 17599-17605, https://doi.org/10.1016/j.ijhydene.2012.04.053.
5. L.C.Shirvill, T.A.Roberts, M.Royle, D.B. Willoughby, P.Sathiahd, Effects of congestion and confining walls on turbulent deflagrations in a hydrogen storage facility-part 1: Experimental study, International Journal of Hydrogen Energy, Volume 43, Issue 15, Pages 7618-7642, https://doi.org/10.1016/j.ijhydene.2018.02.135.
6. Skjold, et al. (2017). Experimental investigation of vented hydrogen deflagrations in containers – Phase 1: Homogeneous mixtures. Report HySEA-D2-04-2017, July 2017: 304 pp.
7. Skjold, et al. (2019). Vented deflagrations in containers: Effect of congestion for homogeneous and inhomogeneous mixtures, International Journal of Hydrogen Energy, Volume 44, Issue 17, Pages 8819-8832. https://doi.org/10.1016/j.ijhydene.2018.10.010
8. Skjold, et al. (2017). Influence of congestion on vented hydrogen deflagrations in 20-foot ISO containers: homogeneous fuel-air mixtures. Twenty-Sixth International Colloquium on the Dynamics of Explosions and Reactive Systems (26 ICDERS), Boston, 30 July – 4 August 2017.
9. Schiavetti M., Pini T., Carcassi M. "Comparison of experimental tests on hydrogen deflagration in homogeneous and non-homogenous condition" The International Symposium of Hydrogen Fire Explosion and Safety Standard (ISHFESS 2018), July 6-8 2018 Hefei, China
10. Skjold T. et al. "Blind-prediction: Estimating the consequences of vented hydrogen deflagrations for homogeneous mixtures in 20-foot ISO containers" International Journal of Hydrogen Energy, Volume 44, Issue 17, Pages 8977-9008.
11. Skjold T. et al. "Blind-prediction: estimating the consequences of vented hydrogen deflagrations for inhomogeneous mixtures in 20-foot ISO containers." Proceedings Twelfth International Symposium on Hazards, Prevention and Mitigation of Industrial Explosions (12 ISHPMIE), ISBN 978-1-5323-8443-1, Kansas City, 12-17 August 2018: 875-898. DOI: https://doi.org/10.5281/zenodo.2600761